

OPEN

Malaria predictions based on seasonal climate forecasts in South Africa: A time series distributed lag nonlinear model

Yoonhee Kim¹, J. V. Ratnam², Takeshi Doi², Yushi Morioka², Swadhin Behera², Ataru Tsuzuki³, Noboru Minakawa³, Neville Sweijid⁴, Philip Kruger⁵, Rajendra Maharaj⁶, Chisato Chrissy Imai^{3,7}, Chris Fook Sheng Ng⁸, Yeonseung Chung^{3,9} & Masahiro Hashizume^{2,8*}

Although there have been enormous demands and efforts to develop an early warning system for malaria, no sustainable system has remained. Well-organized malaria surveillance and high-quality climate forecasts are required to sustain a malaria early warning system in conjunction with an effective malaria prediction model. We aimed to develop a weather-based malaria prediction model using a weekly time-series data including temperature, precipitation, and malaria cases from 1998 to 2015 in Vhembe, Limpopo, South Africa and apply it to seasonal climate forecasts. The malaria prediction model performed well for short-term predictions (correlation coefficient, $r > 0.8$ for 1- and 2-week ahead forecasts). The prediction accuracy decreased as the lead time increased but retained fairly good performance ($r > 0.7$) up to the 16-week ahead prediction. The demonstration of the malaria prediction process based on the seasonal climate forecasts showed the short-term predictions coincided closely with the observed malaria cases. The weather-based malaria prediction model we developed could be applicable in practice together with skillful seasonal climate forecasts and existing malaria surveillance data. Establishing an automated operating system based on real-time data inputs will be beneficial for the malaria early warning system, and can be an instructive example for other malaria-endemic areas.

Malaria is a life-threatening infectious disease caused by parasites transmitted to human through a mosquito vector. Effective malaria control strategies have decreased the burden of malaria in recent decades. Globally, an 18% reduction in malaria incidence was estimated from 2010 to 2017¹. However, there is still much uncertainty in the decline of the malaria burden because of spatial heterogeneity and temporal change², and a high burden is still being reported. In 2017, global estimates of 219 million new malaria cases and 451,000 deaths by malaria were reported¹.

The World Health Organization (WHO) African Region was estimated to have the most substantial burden of malaria, accounting for 92% of malaria cases in 2017¹. In South Africa, malaria cases have occurred predominantly in three provinces in the north and northeast (KwaZulu-Natal, Limpopo, and Mpumalanga) near the borders with Mozambique, Zimbabwe, and Botswana. The South African government has the aim of eliminating malaria by 2020, which is a common goal among the Elimination 8 Regional Initiative countries³. The number of malaria cases in South Africa decreased gradually from 8,060 in 2010 to 1,157 in 2015, but resurged in 2016 and reached 22,517 cases in 2017¹.

Malaria is sensitive to climate. Rainfall and temperature are considered the main weather factors that highly determine malaria epidemics⁴. High rainfall increases the number of breeding sites for mosquitoes and leads

¹Department of Global Environmental Health, Graduate School of Medicine, The University of Tokyo, Tokyo, Japan.

²Application Laboratory, Japan Agency for Marine-Earth Science and Technology, Yokohama, Japan. ³Institute of Tropical Medicine, Nagasaki University, Nagasaki, Japan. ⁴Alliance for Collaboration on Climate and Earth Systems Science, Cape Town, South Africa. ⁵Department of Health, Limpopo, South Africa. ⁶Office of Malaria Research, Medical Research Council, Durban, South Africa. ⁷Australian Institute of Health Innovation, Macquarie University, Sydney, Australia. ⁸School of Tropical Medicine and Global Health, Nagasaki University, Nagasaki, Japan.

⁹Department of Mathematical Sciences, Korea Advanced Institute of Science and Technology, Daejeon, Republic of Korea. *email: hashizume@nagasaki-u.ac.jp

to increases in malaria transmission. Some studies, however, have reported that intense rainfall could flush early-stage larvae and shrink mosquito populations in the short term⁵. High temperatures increase the chance of transmission by shortening the duration of parasite growth in mosquitoes⁶. Temperature changes also influence the development, reproduction, survival, and biting rate of mosquitoes^{7–9}.

A malaria early warning system (MEWS) has been considered as a promising tool to prevent/reduce the burden of malaria by accounting for the complexities in the malaria–climate dynamics often changing unexpectedly. Basic elements for a MEWS should include case surveillance (early detection of epidemics), an early warning based on meteorological conditions, and seasonal climate forecasts¹⁰. A robust MEWS not only requires linking the basic elements such as the monitoring/predicting information described above, but should also be based on the high quality of elements that are expected to be persistent and well-organized. In addition, a malaria prediction model that performs accurately together with a high quality malaria surveillance system and high quality seasonal climate forecasts is required to establish a successful MEWS.

Although several MEWSs have been developed^{11,12}, no sustainable system has remained because of several operational difficulties. Previous studies have proposed malaria forecasting methods based on different modeling approaches such as statistical modeling (e.g., generalized linear model (GLM) and autoregressive integrated moving average (ARIMA) time series model), mathematical modeling (e.g., susceptible-exposed-infected-recovered (SEIR) model), and machine learning methods (e.g., neural network)¹³. However, no one method has been a gold standard because each method has different modeling assumptions and the optimal choice of the method depends upon the characteristics of a study population. Another challenge to implement a MEWS in practice may be the great computational burden for obtaining seasonal climate forecasts periodically. Only few studies, for example, in Botswana, West Africa, and India have attempted to demonstrate malaria forecasting by integrating their malaria prediction models with seasonal hindcasts of meteorological variables^{14–16}.

In South Africa, the malaria surveillance system has been operating effectively over the past few decades¹⁷, as malaria is one of notifiable diseases. Although South Africa is regarded as a hypo-endemic malaria area, the relatively well-established malaria surveillance system could be an instructive example to develop a malaria prediction model for use in a MEWS. In this study, we accessed the malaria surveillance database in Vhembe, Limpopo Province to develop a weather-based malaria prediction model for the area, which accounts for more than 60% of the malaria burden in South Africa¹⁸. We applied a flexible statistical modeling approach, a GLM with a distributed lag nonlinear structure, to understand the complexity of nonlinear and delayed malaria-weather associations and develop a weather-based malaria prediction model accordingly. We also demonstrated the malaria prediction model performance based on seasonal climate forecasts to determine if the prediction model could feasibly be used in practice.

Methods

Malaria surveillance data. We obtained malaria data of patients in Vhembe, Limpopo, South Africa from 1 January 1998 to 31 May 2015 that were collected by the surveillance system of the Limpopo Department of Health Malaria Program. All malaria cases recorded in the surveillance system were based on positive blood test results, either through microscopy or a malaria rapid diagnostic test. Clinically diagnosed cases without a positive blood test were excluded from the surveillance system. The surveillance data also included demographic characteristics (e.g., sex and age), date of each case reported, type of malaria parasite, and survey type (passive notification or active survey). The active survey was implemented for the targeted villages only if a malaria case was reported, so makes up only 5% of the surveillance data.

Meteorological observed reanalysis data. We considered two meteorological variables for use in the malaria prediction model: (1) precipitation and (2) ambient temperature. The daily time series of the meteorological variables for the same period as the malaria data were obtained from sources that could provide the data almost in real-time. The observed or estimated daily precipitation was derived from the African Rainfall Climatology, version 2 (ARC2) dataset that combines data from the National Oceanic and Atmospheric Administration (NOAA)/National Center for Environmental Prediction (NCEP)/Climate Prediction Center (CPC) Famine Early Warning System Network (FEWS-NET)¹⁹. The data can be downloaded from <https://iridl.ldeo.columbia.edu/SOURCES/NOAA/NCEP/CPC/FEWS/Africa/DAILY/ARC2/daily/index.html>. The horizontal resolution of the precipitation was $0.1^\circ \times 0.1^\circ$ (about $10 \text{ km} \times 10 \text{ km}$). We also obtained the 2-m ambient temperature observed/estimates from the NCEP-National Center for Atmospheric Research (NCAR) reanalysis²⁰, which is available at <https://www.esrl.noaa.gov/psd/data/gridded/data.ncep.reanalysis.html>. The horizontal resolution of the temperature was $2.5^\circ \times 2.5^\circ$ (about $250 \text{ km} \times 250 \text{ km}$). We averaged the precipitation and the 2-m air temperature over the regions covered in our study area (22.3°S to 23.0°S and 29.2°E to 30.6°E).

Retrospective seasonal climate forecasts. The retrospective seasonal climate forecasts for daily precipitation and 2-m ambient temperature across the regions described above were derived from the dynamically downscaled forecasts of the Scale Interaction Experiment-Frontier Research Center for Global Change, version 2 (SINTEX-F2) Coupled ocean–atmosphere General Circulation Model (CGCM). The data were obtained for the sub-annual period of July–April over the whole study period (1998–2015), which covered endemic malaria seasons in the study area. We used the Weather Research and Forecasting (WRF) model for the dynamical downscaling²¹ so that the horizontal resolution of the SINTEX-F2 CGCM forecasts at $1.1^\circ \times 1.1^\circ$ (about $120 \text{ km} \times 120 \text{ km}$) was downscaled at $9 \text{ km} \times 9 \text{ km}$. We also corrected the systematic bias in simulating atmospheric circulation before implementing the dynamical downscaling²² according to previous studies that demonstrated improved SINTEX-F2 forecasts in the southern African region^{23,24}. The SINTEX-F2 system can predict climate variability not only in the tropical Pacific but also in tropical and subtropical Indian Ocean, which can work as potential

sources of seasonal predictability over southern Africa. Details of the SINTEX-F2 CGCM forecasts (e.g., model set-up, forecasting experiments, and prediction skills) have been described elsewhere^{25,26}.

Statistical analysis. We aggregated the datasets described above (i.e., individual malaria surveillance data, the daily time series of the weather observations, and the seasonal climate forecasts) to weekly time series for statistical analysis. To obtain the same number of weeks every year (1–52 weeks), we constructed the weekly data starting on 1 January for each year, so the last 1–2 days corresponding to the 53rd week were excluded from our analyses.

The statistical analysis had three main parts: (1) model building to understand the nonlinear and delayed malaria-weather associations and develop a weather-based malaria prediction model accordingly, (2) testing the prediction model based on the reanalysis weather observations assuming perfect weather forecasts, and (3) demonstrating the prediction process based on the bias-corrected and downscaled SINTEX-F2 seasonal climate forecasts appended to the most recent available weather observations.

Model building. We fitted a GLM with a Poisson family taking into account over-dispersion. We considered a distributed lag nonlinear structure to investigate the nonlinear and nonlinearly-delayed associations between malaria incidence and weather factors²⁷. The distributed lag nonlinear model (DLNM) has been used widely in studies that examined the association between environmental exposure and health outcome, for example, the temperature-mortality association²⁸ and the climate-dengue association²⁹. Specifically, we incorporated a cross-basis function for the temperature-malaria association in the model, characterized by a quadratic B-spline with an internal knot at the 50th percentile of temperature and a natural cubic spline for a lag of 0–12 weeks with two internal knots equally-spaced on a log scale. We chose the maximum lag of 12 weeks using the lag-response curve for the temperature-malaria association in which the period of 0–12 weeks was long enough to capture the increased risk of malaria for temperature as well as the decreased displacement pattern of the risks.

To examine the association between precipitation and malaria incidence, we used a simpler approach than the distributed lag nonlinear structure to minimize the correlation between temperature and precipitation terms that tended to result in high uncertainty in malaria predictions. We also considered different lag periods of precipitation under the hypothesis that short and long delayed effects of precipitation may have independent roles. We applied two nonlinear functions of the short- and long-term averages of precipitation (from the current week to the preceding 15 weeks and 51 weeks, respectively) using a natural cubic spline with 5 and 3 degrees of freedom, respectively, after a natural log transformation due to the skewness of the distribution.

We also added a linear term of the previous malaria cases at the preceding week after transforming it by a natural logarithm. This additional term is regarded as a risk factor based on the general feature of infectious disease (i.e., the vector–host–vector transmissions in our study), and incorporating the term could reduce the serial auto-correlation in the residuals of the model³⁰. Another linear term of the year was also included in the model to adjust for the long-term declining trend of malaria incidence. The model framework and equations are provided in the Supplementary Information. The modeling choices were tested in sensitivity analysis, described in the separate section below.

From the model fit, we estimated the associations between malaria incidence and weather factors as a relative risk (RR) indicating a risk for the exposure levels compared with that at a reference value. In our study, we set the reference point as the values representing the minimum estimated risk of malaria incidence for temperature and 1-year average of precipitation (i.e., 12.1 °C and 2.0 on the log scale, respectively). We also used zero (log scale) as a reference for the 4-month average precipitation.

We compared four models including a different combination of the covariates as follows: Model 1, temperature only; Model 2, two covariates representing short- and long-term precipitations; Model 3, temperature and the two precipitation terms; and Model 4, addition of the previous malaria cases to Model 3.

Testing the prediction model based on the weather observations. Using the DLNM, we predicted the (retrospective) future number of malaria cases for 1–16 weeks to evaluate the model's prediction performance. We used the observed temperature and precipitation data as the forecast information (perfect forecast) to examine the performance to avoid involving the uncertainty of the climate prediction. We employed a self-updating process to generate values for the auto-correlation terms in the model. Specifically, we predicted the number of malaria cases one week ahead using the observed weather data. This first 1-week-ahead prediction of malaria cases was then regarded as the auto-correlation term in the subsequent model to obtain the second 1-week-ahead prediction of malaria cases. Next, the first and second 1-week-ahead predictions were used to compute the third 1-week-ahead prediction, and so on until the sixteenth 1-week-ahead prediction was obtained.

To demonstrate a real-time weekly-updated prediction process, we used subsets of data (9 years; approximately 50% of the data) to build the DLNM and obtain the (retrospective) future malaria prediction for the forecasting periods (the following 1–16 week). We moved the 9-year data window forward week by week, which generated a total of 416 iterations (Supplementary Fig. S1).

Accuracy of the malaria prediction models. We used several measures to assess the accuracy of the malaria prediction model. First, we calculated the Spearman correlation coefficient between the observed and predicted malaria cases. Second, we calculated the root mean square error (RMSE); the equation of the RMSE is described in the Supplemental Information. Third, we calculated the area under the curve (AUC) of the receiver operating characteristic (ROC). To do this, we defined an outbreak of malaria using a level of the threshold at the 40th percentile of the past moving 5-years malaria cases during the endemic season (September–May). We chose the threshold level of the 40th percentile by taking into account the AUC values by different levels of the threshold from the 40th to the 80th percentiles (Supplementary Fig. S2). Fourth, we calculated a concordance rate (%), defined

by the ratio of the sum of true positive and true negative values (weeks) to the total number of weeks. Lastly, we calculated sensitivity and specificity. The sensitivity was defined as the ratio of the number of predicted outbreaks to the number of true observed outbreaks. The specificity was defined as the ratio of the number of predicted non-outbreaks to the number of true observed non-outbreaks. All the accuracy measures were calculated for each lead time of 1–16 week ahead over the iterations described in the previous section above.

Demonstrating the prediction model based on seasonal climate forecasts. To demonstrate the implementation of the malaria prediction model in a real setting, we modified the weekly-updated prediction process described above by replacing the observed weather data with the seasonal climate forecasts produced by the dynamical downscaled SINTEX-F2. Because we considered the delayed effects of temperature and precipitation in the DLNM, we used a hybrid of weather data consisting of observed values and climate forecasts at a certain time point for the malaria predictions. Also, although the observed weather data can be provided in almost real time, we supposed that the seasonal climate forecasts could be updated only once a month because of the heavy computational cost. Thus, the same climate forecast data were used for the weekly-updated malaria predictions (retaining the same lead time of 1–16 weeks) until the following month when the next updates of climate forecasts were provided. The time periods of this test were shorter from July to April than for the time periods that used the observed weather data because of the availability of the seasonal climate forecasts.

Sensitivity analysis. We altered the DLNM specification and chose the best models with higher levels of prediction performance using the accuracy measures described above: correlation coefficients, RMSE, concordance rate, and the AUC (Supplementary Fig. S3). First, we changed the degree of freedom (df) for the associations between malaria incidence and the short- and long-term averages of precipitation from 2 to 6 and from 1 to 5, respectively. Second, we changed the number of internal knots for the temperature–malaria association from 1 to 3. Third, we changed the functional form of the auto-correlation terms: (1) a single lag of preceding week as a linear term, (2) a single lag of preceding week as a natural cubic spline with 3 df, (3) a moving average of preceding 1–4 weeks as a natural cubic spline with 3 df, and (4) a cross-basis function including a quadratic B-spline with a knot at the 50th percentile of the preceding 1–4 weeks and a natural cubic spline for the nonlinear distributed lags with a knot at equally-spaced log value. Lastly, we changed the lag periods of the short-term average of precipitation from 0–4 weeks to 0–24 weeks.

All analyses were performed using R version 3.5.1 with the packages “dlnm” for the distributed lag nonlinear models and “pROC” for the AUC calculations.

Results

A total of 53,689 patients who were diagnosed with malaria were included in the present study. Mean age of the patients was 25.2 years (standard deviation (SD) = 17.7); 55.2% were male and 44.8% were female. The *Plasmodium falciparum* was predominant among the infected patients (99.6%). It was identified by a definitive diagnosis using either a malaria rapid diagnostic test or a microscope blood smear. The fatality rate was 1.0% (534 patients).

Figure 1 shows the weekly time series of malaria patients, mean 2-m air temperature, and total precipitation in the study area. The average weekly number of patients with malaria was 59 (SD = 72), and, in general, the numbers decreased over time. The malaria incidence also showed clear seasonal fluctuations with higher levels in warm and rainy seasons (average = 76 and SD = 75 during September–May) and lower levels in cool and dry seasons (average = 7 and SD = 8 during June–August). The average weekly temperature was 20.6 °C (SD = 3.7 °C) over the years, and it ranged from 12.1 °C to 27.9 °C. The average weekly total precipitation was 9.7 mm (SD = 20.5 mm); however, the distribution of the precipitation was skewed because of heavy rainfalls, particularly in 1999–2000 and 2012–2013.

Associations of malaria incidence with weather factors. Figure 2 shows the associations between weather factors and malaria incidence. For the association with temperature, nonlinear and delayed patterns were obvious over the 0–12 lag weeks adjusting for precipitation (see also the 3D plot in Supplementary Fig. S4). Specifically, we found that the relative risk (RR) for temperature at lag of 2 weeks increased with increasing temperature, but reached the highest level of RR at moderate temperatures (approximately 23–24 °C) and then decreased at higher temperatures (Fig. 2A). The RR for 24 °C was highest at lag of 2 weeks (Fig. 2B).

The shape of curves for precipitation varied between the 4-month and 1-year averages (Fig. 2C,D). The RR for the 4-month average of precipitation increased as the weekly total precipitation increased up to approximately 20 mm (equal to 3 on the log scale) (Fig. 2C), then decreased at higher precipitation, which may be explained by the washing out the breeding sites of mosquitoes by heavy rainfalls. The washing-out effect may be temporary during a couple of months because, for the higher levels of the long term 1-year average of precipitation, the malaria incidence increased (Fig. 2D).

Accuracy of the prediction models. Figure 3 shows the malaria prediction accuracy over the lead time among Models 1–4 from the weekly-updated prediction process using the observed weather data (assuming perfect weather forecast) for each of the accuracy measures (Spearman correlation coefficient, RMSE, concordance rate, AUC, sensitivity, and specificity). We found that Model 1 with the cross-basis function of temperature over the lag of 0–12 weeks captured the seasonal fluctuations of malaria transmission fairly well. However, the prediction accuracy was much improved after adding the 4-month and 1-year averages of precipitation to the model (Model 3). In Model 4, adding the auto-correlation term generally improved the short-term predictions for the 1–3 week lead time, particularly in the results of correlation coefficient, concordance rate, and AUC, although

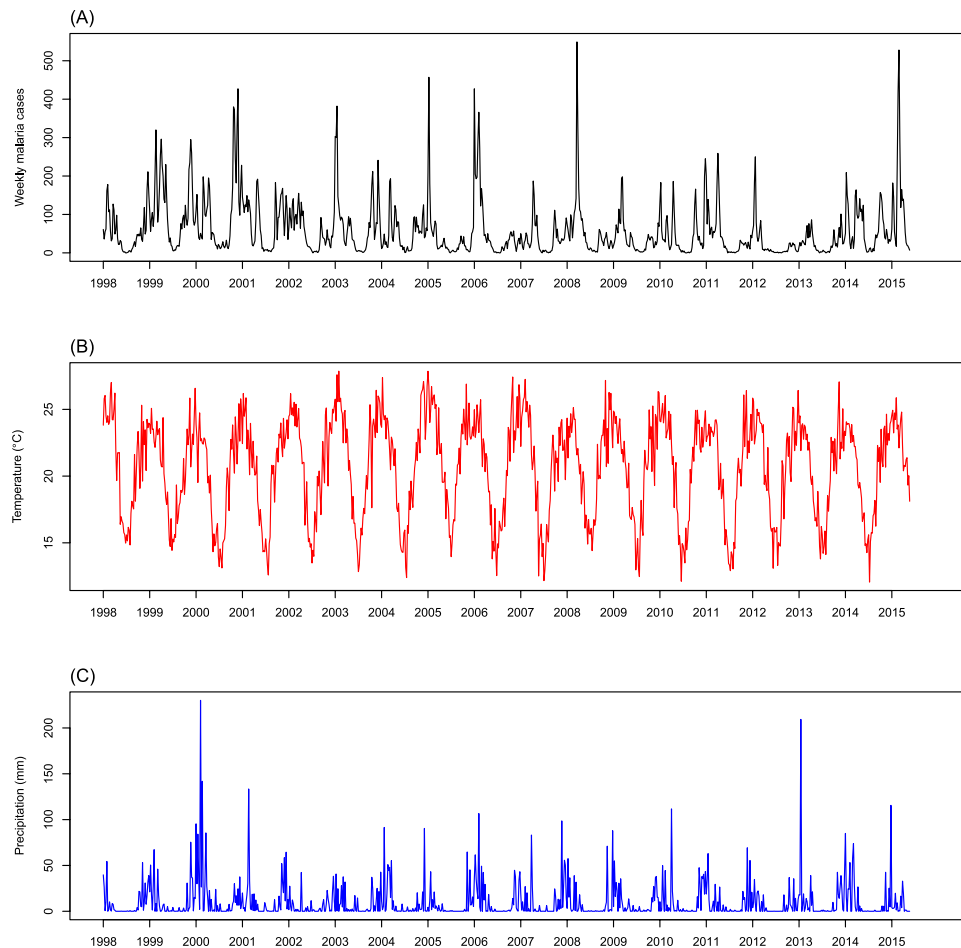


Figure 1. Weekly time series of (A) malaria cases, (B) mean 2-m air temperature (°C), and (C) total precipitation (mm) in Vhembe district, Limpopo Province, South Africa.

it showed slightly higher RMSE and lower specificity for longer-term predictions. We chose Model 4 as the best model to demonstrate the weekly-updated prediction process based on seasonal climate forecasts.

Malaria predictions based on the seasonal climate forecasts. Figure 4 shows the cumulative annual number of malaria incidences and malaria outbreaks for the 2-weeks-ahead lead time, selected from among the 1- to 16-weeks-ahead predictions. Overall, the 2-weeks-ahead prediction values coincided closely with the observed values, although they tended to be higher at the first four years out of eight years (Fig. 4A). The biggest gap between prediction and observation was during the 2014–2015 season, probably because the prediction model did not detect the huge outbreak in early 2015 (Supplementary Fig. S5-A). The trend of the number of outbreaks was consistent with the number of malaria incidences in general (Fig. 4B). However, these results somewhat varied depending on how to define the outbreak (Supplementary Fig. S6). We also provided the additional results for the 4-weeks-ahead predictions and observations in Supplementary Figs. S5-B, S7.

Discussion

In this study, we developed a weather-based malaria prediction model using a flexible statistical approach that takes into account the nonlinear and delayed associations between malaria transmission and climate factors. The malaria prediction model showed good performance particularly for short-term predictions for 1- and 2-weeks ahead. The accuracy of the prediction decreased as the lead time increased, but retained fairly good performance up to 16-weeks ahead.

In the demonstration of the weekly-updated malaria prediction process using the dynamically downscaled seasonal climate forecasts, we also found that the short-term prediction values coincided closely with the observed values. To our best knowledge, a limited number of previous malaria prediction models used the seasonal climate forecasts that are required to implement such models in a real setting together with the malaria surveillance data^{14–16}. The weekly-updated malaria prediction process demonstrated in our study would be merited if it is implemented in the local communities in Limpopo province, South Africa, which could provide better opportunities for public health practice such as improving decision making for the optimal deployment of resources (e.g., timely distribution of drugs and/or higher impact of malaria control interventions by more efficient scheduling of indoor residual spraying)¹.

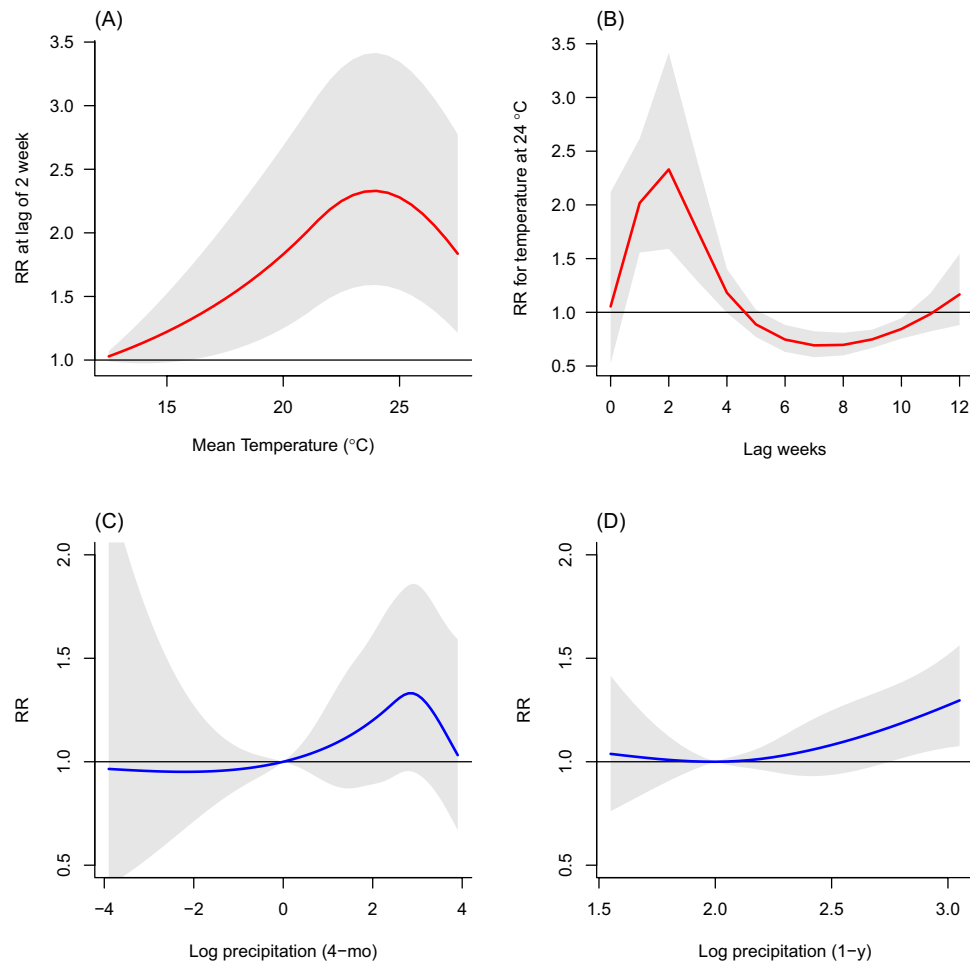


Figure 2. Associations between malaria incidence and weather factors. The relative risks (RR) for temperature (A) at lag of 2 weeks and (B) the lag-response curve for 24 °C, and the RR for the log precipitation of (C) 4-month (4-mo) and (D) 1-year (1-y) averages.

Our results for the association with temperature showed that the malaria risk was highest at moderate temperatures (approximately 23–24 °C as a weekly average) at lag of 2 weeks and decreased at lower or higher temperatures, although the risk was higher at extremely high temperatures (27.9 °C) than at extremely low temperatures (12.0 °C). Previous studies suggested there may be a critical temperature range for mosquito survival, and the longevity of mosquito vectors could be shortened at extremely high temperatures^{7–9,31}. In our study, we observed a clear lag pattern for the malaria–temperature association. Significant higher risk persisted during lag of 1–4 weeks with the peak at lag of 2 for the moderate temperature (24.0 °C), followed by lower risk at lag of 6–10 weeks. The higher risk at the shorter lag periods seem reasonable when taking into account the overall lengths of the lifecycle of the malaria parasite (particularly for the incubation period in a human host) and gonotrophic cycle for vector mosquitoes. It is known that the incubation period from malaria infection by mosquito bite (sporozoites injected to human host) to when symptoms appear is an average of 12–14 days³². The gonotrophic cycle takes a few days but is highly dependent on the temperature; high temperatures can shorten the cycle and lead to an increase in the mosquito population³³. The lower risk at longer lag periods seem to reflect the ‘harvesting’ phenomenon, an epidemiological term that describes the displacement of mortality after episodes of high temperature that temporarily reduce susceptible populations³⁴. This could be explained by changes in the human host population attributable to the large risk increases in the early period of our study. However, the mechanism for the longer lag temperature effects on malaria based on epidemiological evidence is unclear. Different mechanisms besides displacement may exist to explain the harvesting-like lag pattern.

The nonlinear associations for precipitation were investigated using smooth functions of the average of preceding 4-month and 1-year weekly totals (reflecting sub-seasonal and longer-term precipitations, respectively). These smooth functions were simpler than the cross-basis function applied to temperature in terms of the number of parameters accounting for the exposure–response association and corresponding lag structure simultaneously. In general, evaluating the influence of precipitation on vector lifecycle is more variable and more uncertain than evaluating it with the temperature effects³³. Also, the uncertainty of the seasonal climate forecasts for precipitation is generally larger than for temperatures^{25,35}. We believe that our simpler approach could be beneficial to reduce the uncertainties potentially added up by different sources (i.e., the association for precipitation and the predicted precipitation described above) in the process of predicting malaria incidence. Nevertheless, we

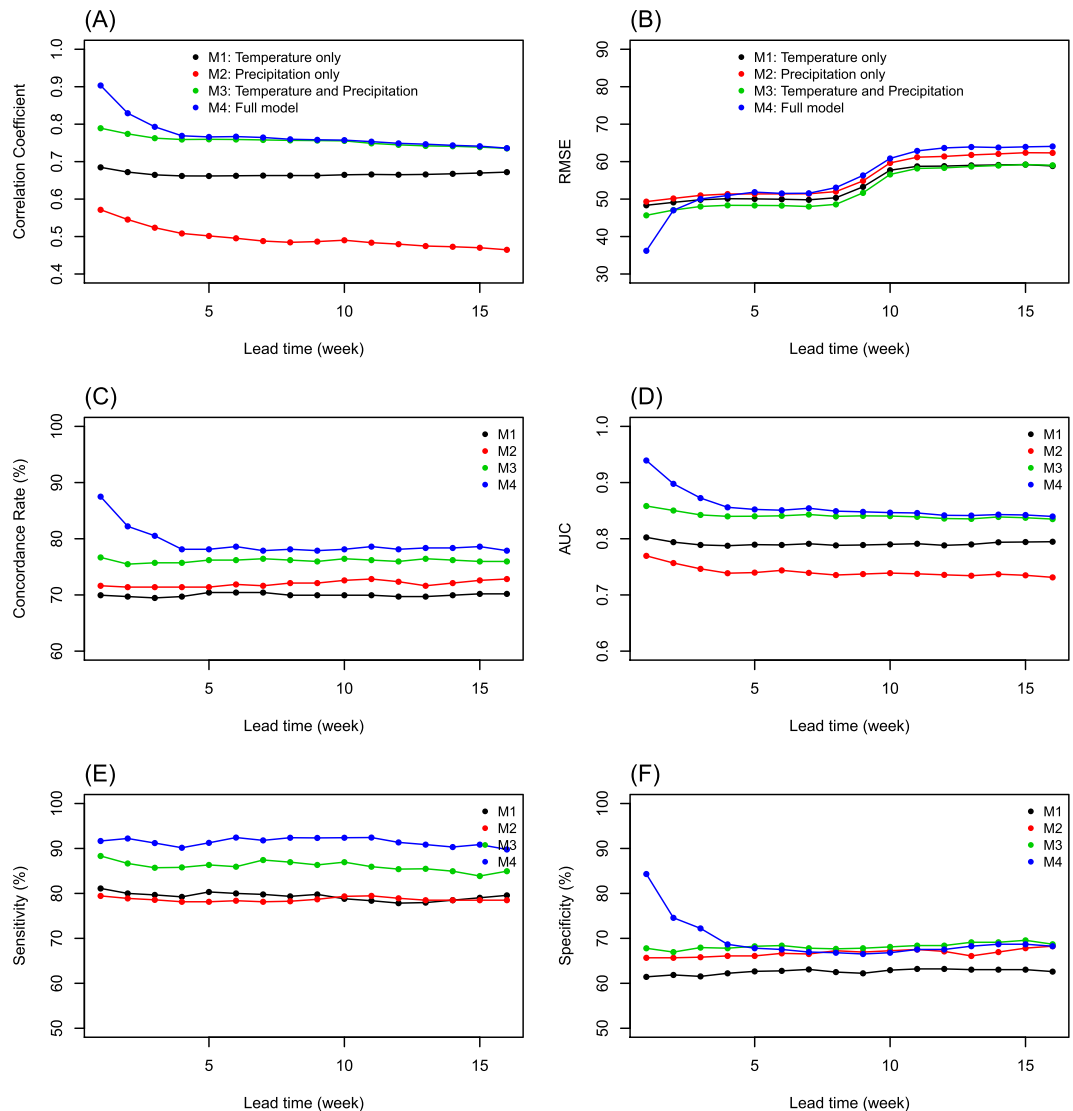


Figure 3. Prediction accuracy over lead time (week) using four different models. Model 1 (M1), temperature only; Model 2 (M2), short- and long-term precipitations only; Model 3 (M3), temperature and two precipitations; and Model 4 (M4), all variables with addition of the previous malaria cases from the weekly-updated malaria prediction process based on the observed weather data (assuming perfect weather forecasts). The accuracy measures were (A) Spearman correlation coefficient, (B) root mean square error (RMSE), (C) concordance rate (%), (D) area under the curve (AUC) of the receiver operating characteristic (ROC), (E) sensitivity (%), and (F) specificity (%).

considered two different time scales of the precipitation to take into account the complex dynamic of mosquito populations associated with precipitation and thus their breeding sites as much as possible. The shapes of the curves for the sub-seasonal and longer-term precipitation varied considerably (Fig. 2C,D). The results suggest that persistence of breeding sites is less likely with high amount of precipitation caused by frequent heavy rainfalls within a season^{5,36}, whereas higher annual precipitation in a preceding year may influence the hydrological environment overall in terms of the number of breeding sites, possibly related to soil moisture and vegetation in a longer-term perspective³⁷. A previous modeling study reported that annual precipitation accounted for only 60% of the variance in adult mosquito populations in a Niger Sahel village in Africa, and the mosquito abundance was better explained by incorporating intra-seasonal rainfall variability and the simulated surface area of standing water than by annual precipitation alone³⁶. Also, a 21-years cohort study using the Health and Demographic Surveillance System (HDSS) data in Agincourt in South Africa, which is located in the neighboring province of our study location (approximately 350 km away), reported that the increased risk of malaria mortality was significantly associated with both higher yearly rainfall and the joint effects of monthly rainfall–temperature, which adjusted each other in the model³⁸.

Although our prediction model showed good performance for short-term malaria predictions in general, we recognized that the predictions incorporating the seasonal climate forecasts were largely underestimated for the

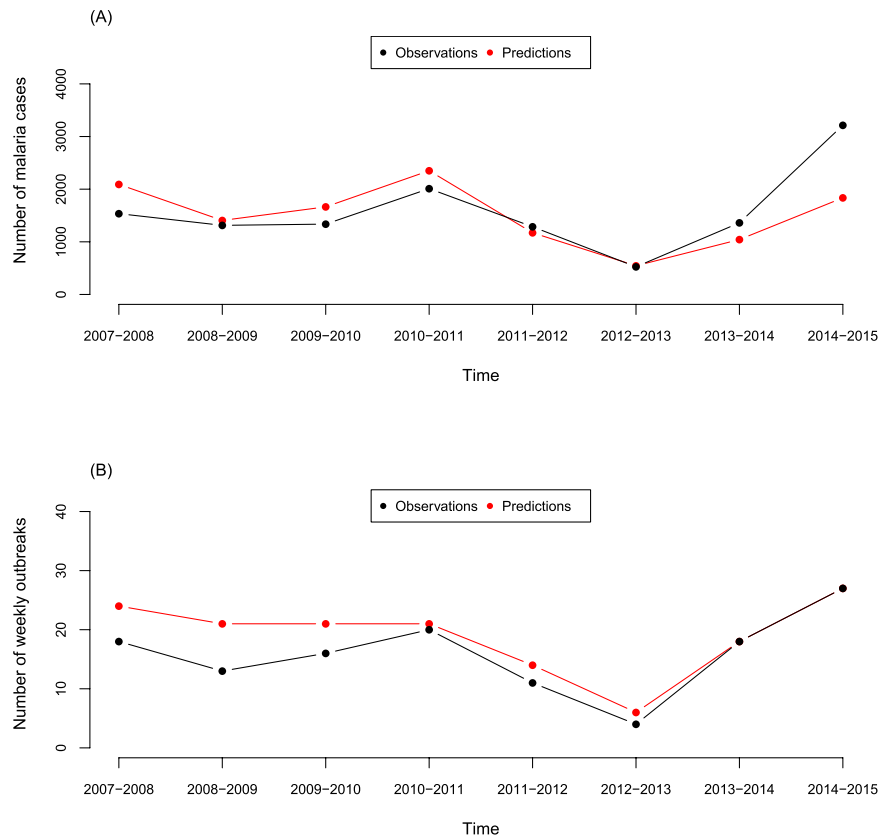


Figure 4. Cumulative annual number of malaria incidence and malaria outbreaks, defined by the 40th percentile of the past moving 5-years malaria cases during the endemic season (September–May), for the 2-weeks-ahead lead time (red, predictions; black, observations) in the demonstration of the weekly-updated malaria prediction process based on seasonal climate forecasts.

2014–2015 season, even the 2-weeks-ahead prediction results (Fig. 4A). The low accuracy for this season was due mainly to the unexpected huge outbreak that occurred during the 8th–10th weeks in early 2015 (418, 528, and 291 cases, respectively). The precipitations did not seem to greatly contribute to this huge outbreak because the cumulative precipitation totals before the outbreak were lower (245.4 mm from the 35th week of 2014 to the 7th week of 2015) than the average in previous years (335.4 mm for the same week periods since the 2000–2001 season). Some unmeasured/unknown factors other than weather conditions might have played a role to facilitate the malaria transmission in early 2015. In Vhembe, the local cases have been predominant for the malaria burden¹⁸, which was observed consistently in our study in general (Supplementary Fig. S8). However, there was a sudden increase in the proportion of imported malaria cases during the two preceding seasons, 2012–2013 and 2013–2014. We speculate that an increase in the movement of people from areas with higher malaria prevalence outside of the country into Vhembe may have increased the risk of malaria transmission in the 2014–2015 season. Future studies, in collaboration with neighboring countries, to investigate how the interplay between the cross-border transmission and climate factors works are warranted to ultimately achieve the goal of the Elimination 8 Regional Initiative countries³.

We acknowledge some limitations in this study. First, we considered two weather factors (temperature and precipitation) and malaria transmission at a preceding week as only factors taken into account in our prediction model because of data availability of the seasonal climate forecasts, although other climatic factors such as relative humidity and normalized difference vegetation index (NDVI) have been used in the previous studies aiming to develop a malaria prediction model¹³. Second, we did not incorporate the potential role of temporal changes in the immunity levels to malaria when developing our prediction model, which may help to improve the malaria predictions in future studies. Third, our seasonal climate forecasts by the climate prediction models (SINTEX-F2) included some uncertainties that may have produced misclassification of the weather exposure to malaria cases. Further improvement of the seasonal forecast system (e.g., initialization, prediction modeling, and ensemble techniques) may generate better inputs for our malaria prediction model, and consequently, the malaria predictions could be more accurate in the future.

Some previous studies have proposed different modeling approaches¹³ for weather-based malaria forecasting such as statistical modeling (e.g., GLM, generalized additive model (GAM)³⁹, and ARIMA model⁴⁰), mathematical modeling (e.g., SEIR model), and machine learning methods (e.g., neural network⁴¹). Each model includes different assumptions and has its advantages and disadvantages. Statistical models such as GLM or GAM have greater interpretability regarding the relationship between weather factors and malaria but may not fully capture

the residual serial correlations. The ARIMA model can represent the features of temporal patterns (i.e., seasonality and autocorrelation) more sophisticatedly but lacks interpretability of weather covariates. Mathematical models are based on a different assumption that individuals are transferred over time among separate compartments of susceptible, exposed, infected, and recovered groups. Although they represent the dynamics of malaria transmission more explicitly, their disadvantages include the difficulty in specifying key parameters, given the nature of deterministic (not stochastic) models and computational complexity. Lastly, the machine learning approach has been useful as it can handle the highly complex relationship with predictors but has suffered from overfitting and poor interpretability¹³. When performing malaria forecasting, the modeling choice should be guided by the assumptions of different methods and the characteristics of a study population. In this research, we adopted a GLM with a distributed lag nonlinear structure to ensure both interpretability and flexibility to describe the nonlinear and nonlinearly-delayed association between weather factors and malaria. To handle the residual correlation issue, we incorporated the auto-correlation term into the prediction model³⁰. In future studies, a comparison of our forecasting method with other methods is warranted, and an ensemble of multiple predictions may achieve the best prediction performance.

In summary, we developed a malaria prediction model taking into account nonlinear and delayed complexities of the malaria–climate dynamics. The prediction model showed good performance for the short-term lead time, and the prediction accuracy decreased as the lead time increased but retained fairly good performance. We also demonstrated the weekly-updated malaria prediction process based on seasonal climate forecasts and found that the malaria predictions for short-term lead time coincided closely with the observed malaria cases. The malaria prediction model we developed is promising because it is feasibly applicable in practice together with the skillful seasonal climate forecasts and existing malaria surveillance system in South Africa. Establishing an automated operating system based on real-time data inputs could potentially be beneficial for the malaria early warning system in Limpopo, South Africa, and can be an instructive example for other malaria-endemic areas.

Received: 31 May 2019; Accepted: 1 November 2019;

Published online: 29 November 2019

References

1. WHO. World malaria report 2018. *World Health Organization*, <https://www.who.int/malaria/publications/world-malaria-report-2018/en/> (2018).
2. Nkumama, I. N., O'Meara, W. P. & Osier, F. H. A. Changes in Malaria Epidemiology in Africa and New Challenges for Elimination. *Trends Parasitol* **33**, 128–140, <https://doi.org/10.1016/j.pt.2016.11.006> (2017).
3. Elimination8. *Elimination 8 Regional Initiative*, <https://malariaelimination8.org/> (2016).
4. Caminade, C. *et al.* Impact of climate change on global malaria distribution. *Proc Natl Acad Sci USA* **111**, 3286–3291, <https://doi.org/10.1073/pnas.1302089111> (2014).
5. Paaijmans, K. P., Wandago, M. O., Githeko, A. K. & Takken, W. Unexpected high losses of *Anopheles gambiae* larvae due to rainfall. *PLoS one* **2**, e1146, <https://doi.org/10.1371/journal.pone.0001146> (2007).
6. Okech, B. A. *et al.* The development of *Plasmodium falciparum* in experimentally infected *Anopheles gambiae* (Diptera: Culicidae) under ambient microhabitat temperature in western Kenya. *Acta Tropica* **92**, 99–108, <https://doi.org/10.1016/j.actatropica.2004.06.003> (2004).
7. Bayoh, M. N. & Lindsay, S. W. Effect of temperature on the development of the aquatic stages of *Anopheles gambiae* sensu stricto (Diptera: Culicidae). *Bulletin of Entomological Research* **93**, 375–381, <https://doi.org/10.1079/BER2003259> (2003).
8. Bayoh, M. N. & Lindsay, S. W. Temperature-related duration of aquatic stages of the Afrotropical malaria vector mosquito *Anopheles gambiae* in the laboratory. *Medical and Veterinary Entomology* **18**, 174–179, <https://doi.org/10.1111/j.0269-283X.2004.00495.x> (2004).
9. Christiansen-Jucht, C. D., Parham, P. E., Saddler, A., Koella, J. C. & Basáñez, M.-G. Larval and adult environmental temperatures influence the adult reproductive traits of *Anopheles gambiae* s.s. *Parasites & Vectors* **8**, 456, <https://doi.org/10.1186/s13071-015-1053-5> (2015).
10. Cox, J. & Abeku, T. A. Early warning systems for malaria in Africa: from blueprint to practice. *Trends Parasitol* **23**, 243–246, <https://doi.org/10.1016/j.pt.2007.03.008> (2007).
11. Mabaso, M. L. & Ndlovu, N. C. Critical review of research literature on climate-driven malaria epidemics in sub-Saharan Africa. *Public Health* **126**, 909–919, <https://doi.org/10.1016/j.puhe.2012.07.005> (2012).
12. Thomson, M. C., Mason, S. J., Phindela, T. & Connor, S. J. Use of rainfall and sea surface temperature monitoring for malaria early warning in Botswana. *Am J Trop Med Hyg* **73**, 214–221, <https://doi.org/10.4269/ajtmh.2005.73.214> (2005).
13. Zinszer, K. *et al.* A scoping review of malaria forecasting: past work and future directions. *BMJ Open* **2**, e001992, <https://doi.org/10.1136/bmjopen-2012-001992> (2012).
14. Thomson, M. C. *et al.* Malaria early warnings based on seasonal climate forecasts from multi-model ensembles. *Nature* **439**, 576–579, <https://doi.org/10.1038/nature04503> (2006).
15. Jones, A. E. & Morse, A. P. Skill of ENSEMBLES seasonal re-forecasts for malaria prediction in West Africa. *Geophysical Research Letters* **39**, L23707, <https://doi.org/10.1029/2012gl054040> (2012).
16. Lauderdale, J. M. *et al.* Towards seasonal forecasting of malaria in India. *Malaria Journal* **13**, 310, <https://doi.org/10.1186/1475-2875-13-310> (2014).
17. Moonasar, D. *et al.* What will move malaria control to elimination in South Africa? *South African Medical Journal* **103**, 801–806, <https://doi.org/10.7196/SAMJ.7445> (2013).
18. Raman, J. *et al.* Reviewing South Africa's malaria elimination strategy (2012–2018): progress, challenges and priorities. *Malaria Journal* **15**, 438, <https://doi.org/10.1186/s12936-016-1497-x> (2016).
19. Novella, N. S. & Thiaw, W. M. African Rainfall Climatology Version 2 for Famine Early Warning Systems. *Journal of Applied Meteorology and Climatology* **52**, 588–606, <https://doi.org/10.1175/jamc-d-11-0238.1> (2013).
20. Kalnay, E. *et al.* The NCEP/NCAR 40-Year Reanalysis Project. *Bulletin of the American Meteorological Society* **77**, 437–472, [https://doi.org/10.1175/1520-0477\(1996\)077<0437:Tnyrp>2.0.Co;2](https://doi.org/10.1175/1520-0477(1996)077<0437:Tnyrp>2.0.Co;2) (1996).
21. Skamarock, W. C. *et al.* A Description of the Advanced Research WRF Version 3. *National Center for Atmospheric Research*. <https://doi.org/10.5065/D68S4MVH> (2008).
22. Ratnam, J. V., Doi, T. & Behera, S. K. Improving austral summer precipitation forecasts of SINTEX-F2 coupled ocean–atmosphere general circulation model over southern Africa by simple bias correction techniques. *Atmospheric Science Letters* **20**, e885, <https://doi.org/10.1002/asl.885> (2019).

23. Ratnam, J. V., Behera, S. K., Doi, T., Ratna, S. B. & Landman, W. A. Improvements to the WRF Seasonal Hindcasts over South Africa by Bias Correcting the Driving SINTEX-F2v CGCM Fields. *Journal of Climate* **29**, 2815–2829, <https://doi.org/10.1175/jcli-d-15-0435.1> (2016).
24. Ratnam, J. V., Doi, T., Landman, W. A. & Behera, S. K. Seasonal Forecasting of Onset of Summer Rains over South Africa. *Journal of Applied Meteorology and Climatology* **57**, 2697–2711, <https://doi.org/10.1175/jamc-d-18-0067.1> (2018).
25. Doi, T., Behera, S. K. & Yamagata, T. Improved seasonal prediction using the SINTEX-F2 coupled model. *Journal of Advances in Modeling Earth Systems* **8**, 1847–1867, <https://doi.org/10.1002/2016MS000744> (2016).
26. Doi, T., Storto, A., Behera, S. K., Navarra, A. & Yamagata, T. Improved Prediction of the Indian Ocean Dipole Mode by Use of Subsurface Ocean Observations. *Journal of Climate* **30**, 7953–7970, <https://doi.org/10.1175/jcli-d-16-0915.1> (2017).
27. Gasparrini, A., Armstrong, B. & Kenward, M. G. Distributed lag non-linear models. *Statistics in medicine* **29**, 2224–2234, <https://doi.org/10.1002/sim.3940> (2010).
28. Gasparrini, A. *et al.* Mortality risk attributable to high and low ambient temperature: a multicountry observational study. *The Lancet* **386**, 369–375, [https://doi.org/10.1016/S0140-6736\(14\)62114-0](https://doi.org/10.1016/S0140-6736(14)62114-0) (2015).
29. Lowe, R. *et al.* Nonlinear and delayed impacts of climate on dengue risk in Barbados: A modelling study. *PLoS medicine* **15**, e1002613, <https://doi.org/10.1371/journal.pmed.1002613> (2018).
30. Imai, C., Armstrong, B., Chalabi, Z., Mangtani, P. & Hashizume, M. Time series regression model for infectious disease and weather. *Environmental research* **142**, 319–327, <https://doi.org/10.1016/j.envres.2015.06.040> (2015).
31. Beck-Johnson, L. M. *et al.* The effect of temperature on *Anopheles* mosquito population dynamics and the potential for malaria transmission. *PLoS one* **8**, e79276, <https://doi.org/10.1371/journal.pone.0079276> (2013).
32. White, N. J. *et al.* Malaria. *Lancet* **383**, 723–735, [https://doi.org/10.1016/s0140-6736\(13\)60024-0](https://doi.org/10.1016/s0140-6736(13)60024-0) (2014).
33. Eikenberry, S. E. & Gumel, A. B. Mathematical modeling of climate change and malaria transmission dynamics: a historical review. *J Math Biol* **77**, 857–933, <https://doi.org/10.1007/s00285-018-1229-7> (2018).
34. Bhaskaran, K., Gasparrini, A., Hajat, S., Smeeth, L. & Armstrong, B. Time series regression studies in environmental epidemiology. *International journal of epidemiology* **42**, 1187–1195, <https://doi.org/10.1093/ije/dyt092> (2013).
35. Kumar, A., Chen, M. & Wang, W. Understanding Prediction Skill of Seasonal Mean Precipitation over the Tropics. *Journal of Climate* **26**, 5674–5681, <https://doi.org/10.1175/JCLI-D-12-00731.1> (2013).
36. Bomblies, A. Modeling the role of rainfall patterns in seasonal malaria transmission. *Climatic Change* **112**, 673–685, <https://doi.org/10.1007/s10584-011-0230-6> (2012).
37. Malahlela, O. E., Olwoch, J. M. & Adjorlolo, C. Evaluating Efficacy of Landsat-Derived Environmental Covariates for Predicting Malaria Distribution in Rural Villages of Vhembe District, South Africa. *EcoHealth* **15**, 23–40, <https://doi.org/10.1007/s10393-017-1307-0> (2018).
38. Byass, P. *et al.* The long road to elimination: malaria mortality in a South African population cohort over 21 years. *Global Health, Epidemiology and Genomics* **2**, e11, <https://doi.org/10.1017/gheg.2017.7> (2017).
39. Sewe, M. O., Tozan, Y., Ahlm, C. & Rocklöv, J. Using remote sensing environmental data to forecast malaria incidence at a rural district hospital in Western Kenya. *Sci Rep* **7**, 2589, <https://doi.org/10.1038/s41598-017-02560-z> (2017).
40. Darkoh, E. L., Larbi, J. A. & Lawer, E. A. A Weather-Based Prediction Model of Malaria Prevalence in Amenfi West District, Ghana. *Malar Res Treat* **2017**, 7820454, <https://doi.org/10.1155/2017/7820454> (2017).
41. Santosh, T. & Ramesh, D. Artificial neural network based prediction of malaria abundances using big data: A knowledge capturing approach. *Clinical Epidemiology and Global Health* **7**, 121–126, <https://doi.org/10.1016/j.cegh.2018.03.001> (2019).

Acknowledgements

This research was carried out for the iDEWS (infectious Diseases Early-Warning System) project supported by SATREPS (Science and Technology Research Partnership for Sustainable Development) Program of JICA (Japan International Cooperation Agency)/AMED (Japan Agency for Medical Research and Development) in Japan and the ACCESS (Applied Centre for Climate and Earth Systems Science) program of NRF (National Research Foundation) and DST (Department of Science and Technology) in South Africa.

Author contributions

Y.K., N.M. and M.H. designed the study. J.V.R. prepared the observed weather data. J.V.R., T.D., Y.M. and S.B. provided the seasonal climate forecasts. A.T., N.M., N.S., P.K. and R.M. provided the malaria surveillance data. Y.K. conducted the statistical analysis with help from C.C.I., C.F.S.N., Y.C. and M.H. Y.K. wrote the main manuscript text and prepared the figures. All authors reviewed the manuscript and contributed to the interpretation of the results.

Competing interests

The authors declare no competing interests.

Additional information

Supplementary information is available for this paper at <https://doi.org/10.1038/s41598-019-53838-3>.

Correspondence and requests for materials should be addressed to M.H.

Reprints and permissions information is available at www.nature.com/reprints.

Publisher's note Springer Nature remains neutral with regard to jurisdictional claims in published maps and institutional affiliations.



Open Access This article is licensed under a Creative Commons Attribution 4.0 International License, which permits use, sharing, adaptation, distribution and reproduction in any medium or format, as long as you give appropriate credit to the original author(s) and the source, provide a link to the Creative Commons license, and indicate if changes were made. The images or other third party material in this article are included in the article's Creative Commons license, unless indicated otherwise in a credit line to the material. If material is not included in the article's Creative Commons license and your intended use is not permitted by statutory regulation or exceeds the permitted use, you will need to obtain permission directly from the copyright holder. To view a copy of this license, visit <http://creativecommons.org/licenses/by/4.0/>.

© The Author(s) 2019